

# Ultralow Chromatic Dispersion Measurement of Optical Fibers With a Tunable Fiber Laser

B. Auguié, A. Mussot, A. Boucon, E. Lantz, and T. Sylvestre

**Abstract**—We describe a novel convenient technique to allow for the accurate measurement of the dispersion coefficients till fourth-order in the zero-dispersion wavelength region of single-mode optical fibers. The proposed method is based on a careful spectral analysis of modulation instability occurring in both normal and anomalous dispersion regime and the associated dispersive waves emitted by soliton fission. It simply requires a high-power tunable continuous-wave fiber laser and an optical spectrum analyzer and is able to retrieve both the sign and magnitude of dispersion coefficients with enhanced precision.

**Index Terms**—Chromatic dispersion, dispersive waves (DWs), four-wave mixing (FWM), modulation instability (MI), optical fibers.

## I. INTRODUCTION

VARIOUS linear techniques have been successfully demonstrated in the past to allow for the accurate measurement of the chromatic dispersion of optical fibers, including pulse delay measurements, frequency-domain or differential phase-shift techniques, and white-light interferometric methods [1]. However, a fast and precise measurement of the chromatic dispersion can also be performed by taking advantage of the interplay between dispersive and nonlinear effects, by measuring for example the parametric four-wave mixing (FWM) conversion efficiency [1], [2]. Recently, modulation instability (MI) has also been applied to chromatic dispersion measurement in both conventional telecommunication and photonic crystal fibers (PCFs) [3]–[5]. Both methods are closely related and fundamentally rely on the underlying phase-matching condition which depends both on the dispersion coefficients and on the nonlinear phase-shift. From an experimental point of view, the latter simply consists of a direct measurement of the MI sidebands by use of a tunable pump laser to retrieve the zero-dispersion wavelength (ZDW) and the group-velocity dispersion (GVD) of optical fibers. However, regarding the FWM phase-matching relation, all dispersion coefficients are strongly correlated close

Manuscript received May 24, 2006; revised June 16, 2006. This work was supported by the Ministère Délégué à la Recherche.

B. Auguié was with Département d’Optique P.M. Duffieux, Institut FEMTO-ST, Université de Franche-Comté, Centre National de la Recherche Scientifique UMR 6174, 25030 Besançon, France. He is now with the Physics Department, University of Exeter, Exeter, Devon EX4 4QL, U.K.

A. Mussot was with Département d’Optique P.M. Duffieux, Institut FEMTO-ST, Université de Franche-Comté, Centre National de la Recherche Scientifique UMR 6174, 25030 Besançon, France. He is now with the Laboratoire de Physique des Lasers, Atomes et Molécules, UMR CNRS 8523, F-59655 Villeneuve d’Ascq, France.

A. Boucon, E. Lantz, and T. Sylvestre are with the Département d’Optique P.M. Duffieux, Institut FEMTO-ST, Université de Franche-Comté, Centre National de la Recherche Scientifique UMR 6174, 25030 Besançon, France (e-mail: thibaut.sylvestre@univ-fcomte.fr).

Digital Object Identifier 10.1109/LPT.2006.881148

to the ZDW point so that it is difficult to extract them independently. In this work, we describe a novel nonlinear technique which scalar MI in both normal and anomalous dispersion regimes and dispersive waves (DWs) emitted by soliton fission. First, scalar MI in the normal dispersion regime indeed allows one to retrieve the fourth-order dispersion coefficient. Second, the third-order dispersion (TOD) can be obtained from the blue-shifted DWs emitted by soliton fission [6]. Based on a nonlinear fitting technique, the proposed method is able to retrieve both the sign and magnitude of higher order dispersion parameters directly from the experimental MI spectra.

## II. THEORY

Let us recall that MI manifests itself in optical fibers as breakup of continuous-wave (CW) high-power laser radiation into a train of ultrashort soliton-like pulses because of the interplay between nonlinearity-induced self-phase modulation and the GVD [7]. In the Fourier domain, MI leads to the growth of two FWM Stokes and anti-Stokes sidebands frequency-shifted by an amount  $\Omega$  from the initial laser frequency  $\omega_p$  according to the phase-matching relation. In the ZDW region of optical fibers, this phase-matching takes the following form [7]:

$$\beta_2\Omega^2 + \frac{\beta_4}{12}\Omega^4 + 2\gamma P = 0 \quad (1)$$

where  $\beta_2$  and  $\beta_4$  are the second and fourth (dispersion curvature) even order dispersion coefficients, respectively, derived from a Taylor expansion of the propagation constant at frequency  $\omega_p$  [7].  $\gamma$  and  $P$  are the nonlinear coefficient and the pump power, respectively. Note that in (1) we do not take into account fiber losses [5]. Depending on the sign and magnitude of  $\beta_2$  and  $\beta_4$  terms, MI can occur under different phase-matching situations that are illustrated in Fig. 1. As shown by the solid line, MI gain does not strictly require anomalous dispersion ( $\beta_2 < 0$ ). Indeed, it can exist in the low normal dispersion regime through negative fourth-order dispersion ( $\beta_4 < 0$ ), as it has been recently demonstrated in both conventional dispersion-shifted fiber (DSF) and PCFs [8]–[10]. On the other hand, if  $\beta_4 > 0$ , MI cannot appear under normal dispersion but presents a branch of two solutions for  $\Omega$  from a certain amount of anomalous dispersion (dashed line).

In addition, it has been shown that a soliton propagating close to the ZDW point is unstable because of higher order dispersion perturbation [11], [12]. In the same way, solitons generated by MI in the CW regime are unstable. They undergo a red-shift and simultaneously shed blue-shifted DWs [6]. These nonsolitonic radiations are frequency-shifted by an amount  $\delta\omega = \omega_{\text{DW}} -$

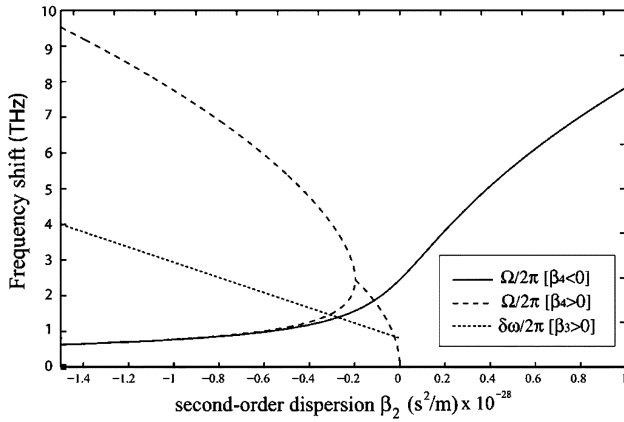


Fig. 1. Phase matching as a function of the second-order dispersion  $\beta_2$  for MI with positive  $\beta_4$  (dashed line) and negative  $\beta_4$  (solid line), respectively, given by (1) and for DWs (dotted line), given by (2). The parameters are  $\beta_3 = 1.15 \cdot 10^{-40} \text{ s}^3 \text{ m}^{-1}$ ,  $\beta_4 = \pm 5.6 \cdot 10^{-55} \text{ s}^4 \text{ m}^{-1}$ ,  $\gamma P = 1 \text{ km}^{-1}$ .

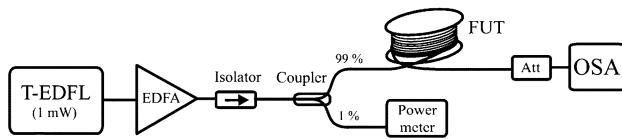


Fig. 2. Experimental setup. T-EDFL: tunable EDFL; Att: Attenuator.

$\omega_p$  from the central soliton frequency  $\omega_p$ , which satisfies the following phase-matching condition [6], [11], [12]:

$$-\frac{\beta_3}{3}\delta\omega^3 + \beta_2\delta\omega^2 - \gamma P = 0. \quad (2)$$

where  $\beta_3$  is the TOD (dispersion slope). The phase-matching for DW is plotted on Fig. 1 as a dotted line and shows a linear dependence with the second-order dispersion. In the following, we will see that combining (1) and (2) with experimental measurements has a potential application for ultralow chromatic dispersion measurement.

### III. EXPERIMENT

The experimental setup is schematically sketched in Fig. 2. The optical fibers under test (FUT) are 3.1-km-long conventional DSFs and 500-m-long highly nonlinear fiber (HNLF), both exhibiting a ZDW close to 1.55  $\mu\text{m}$  but different nonlinear coefficients and dispersion profiles. To generate MI and DW in these standard step-index optical fibers, we use a tunable erbium-doped fiber laser (EDFL) amplified by a high-power erbium-doped fiber amplifier (EDFA) as a pump source. The EDFL is a fiber ring cavity made up of 2-m-long erbium-doped fiber pumped by an 50-mW 980-nm laser diode through a wavelength-division multiplexer, a polarization controller, an optical isolator and a 90/10 output coupler. A tunable optical band-pass filter with 1-nm full-width at half-maximum is inserted in the laser cavity after the fiber coupler to tune the output wavelength from 1530 to 1565 nm around the ZDWs of DSFs. The laser linewidth was measured to 5 GHz using a conventional heterodyne detection technique. It is sufficiently large to ensure that no pump power is backscattered in the DSFs by stimulated Brillouin scattering. With this laser, one additionally takes advantage of its partially coherent nature to seed MI in the DSFs

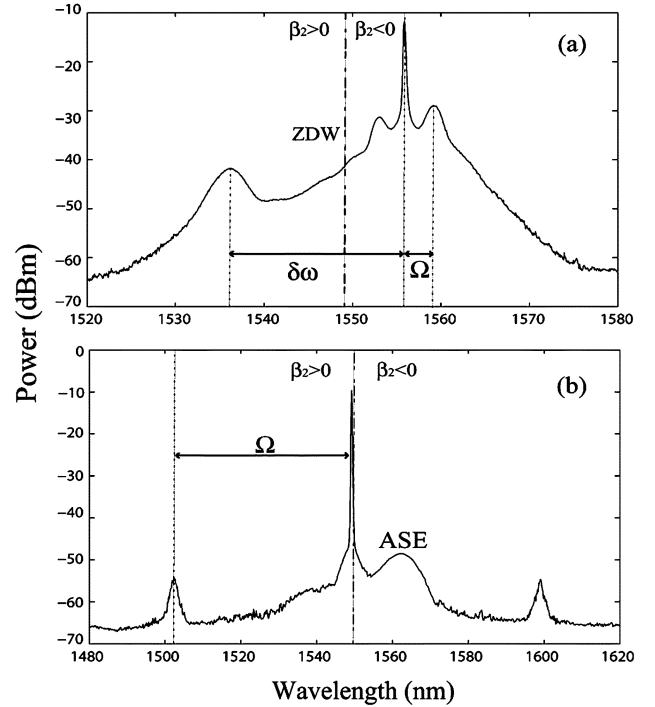


Fig. 3. Experimental output spectra for (a) anomalous and (b) normal dispersion regimes at a pump power of 29 dBm, respectively. The dashed-dotted line indicates the ZDW and the dotted lines indicate the frequency spacing between pump and MI or DW peaks.

through initial phase and amplitude fluctuations [6]. Note, however, that the two narrow MI sidebands may disappear for larger laser linewidth [6]. The EDFL is then amplified by a high-power EDFA (33-dBm output) and coupled to the DSFs by means of a 99/1 fiber coupler. As it can be seen from (1) and (2), the MI and DW frequency-shifts are nonlinearly (pump-power) dependent and it is necessary to precisely assess the input power and the nonlinear coefficient  $\gamma$ . First, input pump power is carefully monitored by means of numerical power meter placed at the 1% arm of the 99/1 coupler, whose wavelength-dependent transmission ratio has been characterized. Second, nonlinear coefficient of the DSF is determined using the technique described in [3]. The output MI spectra are attenuated and recorded using an optical spectrum analyzer with 0.06-nm resolution.

Fig. 3(a) and (b) illustrates the experimental output spectra in the anomalous and normal dispersion regimes, respectively. As it can be clearly seen in Fig. 3(a), two MI sidebands are symmetrically generated around the pump wavelength along with a blue-shifted DW at a shorter wavelength of 1536 nm. Note the power asymmetry between the MI Stokes and anti-Stokes sidebands which is characteristic of the soliton red-shift in the CW pumping regime [6]. For the normal dispersion case, the spectrum of Fig. 3(b) shows the generation of two narrow MI sidebands with larger frequency shift  $\Omega$  due to negative  $\beta_4$ , in complete agreement with solid line of Fig. 1. Note also the presence of a wide Stokes band that is due to the remaining amplified spontaneous emission at the input of the high-power EDFA, which may be suppressed by adding a bandpass optical filter after the EDFA. The  $\Omega$  and  $\delta\omega$  frequency shifts are automatically measured by scanning the pump wavelength in both FUT. The results of all measurements for the conventional DSF are

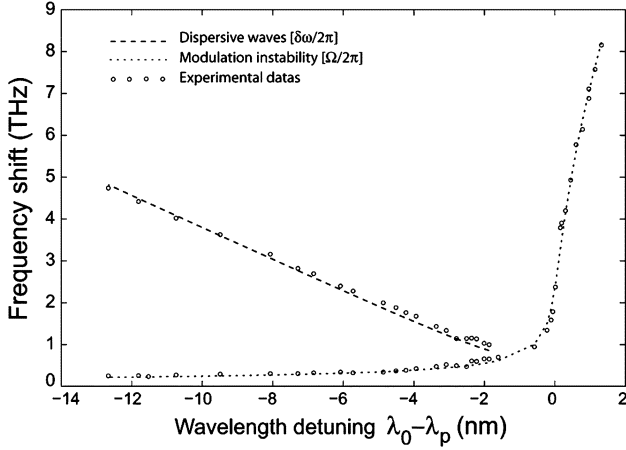


Fig. 4. MI and DWs frequency shifts in function of the pump-ZDW wavelength spacing. Circles: experimental data. Dashed line: nonlinear fit using (2). Dotted line: nonlinear fit using (1).

TABLE I  
MEASURED DISPERSION PARAMETERS WITH ERRORS

| Parameters   | DSF          | HNLF        |
|--|--------------|-------------|
| ZDW(nm)  | 1549.3±0.1   | 1551.4±0.1  |
| Phase-shift  | 1550         | 1552        |
| $D$ (ps.nm <sup>-1</sup> km <sup>-1</sup> )                    | 0.0567       | -0.0453     |
| $\beta_3$ (10 <sup>-40</sup> s <sup>3</sup> .m <sup>-1</sup> ) | 1.15±0.05    | 0.53±0.01   |
| Phase-shift  | 1.15         | 0.5         |
| $D_S$ (ps.nm <sup>-2</sup> km <sup>-1</sup> )                  | 0.071 ± 0.01 | 0.033± 0.01 |
| Phase-shift  | 0.07         | 0.033       |
| $\beta_4$ (10 <sup>-55</sup> s <sup>4</sup> .m <sup>-1</sup> ) | -5.7± 0.1    | -0.65± 0.05 |

reported in Fig. 4 that shows MI and DWs frequency shifts in function of the pump-ZDW wavelength spacing. We can see that  $\delta\omega$  evolves quasi-linearly and that the MI frequency shift exists under normal dispersion, in agreement with the dotted straight line and solid line of Fig. 1.

From all these measurements, we then apply a nonlinear fitting technique based on a classical Gaussian-Newton algorithm which combines (1) and (2) to optimize the values of the three parameters  $\beta_i$  ( $i = 2, 4$ ) and the ZDW. Fig. 4 shows typical fitting curves obtained for the MI and DW frequency shifts in dotted and dashed lines, respectively. One can note a small discrepancy between measurements and fitting curves close to the ZDW, in particular for DWs. To assess the error on the three dispersion parameters, we calculated the associated correlation matrix and checked that these parameters are not strongly correlated, which validates our combined technique. We have also determined the covariance matrix and the standard deviation of the measured parameters. The measured dispersion parameters with errors are reported in Table I for both FUTs in units  $D = -(2\pi c/\lambda_p^2)\beta_2$  and  $D_S = (2\pi c/\lambda_p^2)^2\beta_3$ . Finally, Fig. 5 shows the measured ZDW and GVD coefficient  $D$  for both fibers.

#### IV. CONCLUSION

A convenient technique for ultralow chromatic dispersion measurement of optical fibers has been reported. Based on

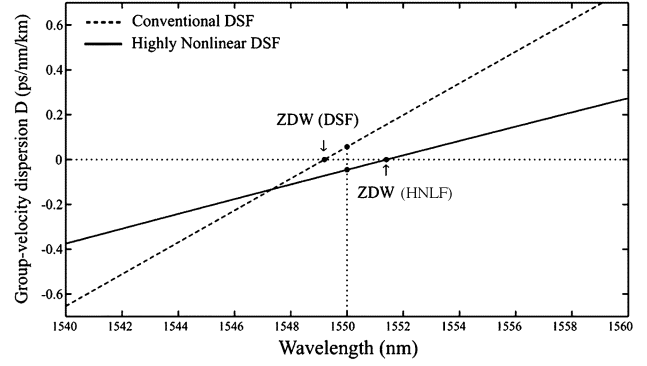


Fig. 5. Measured GVD parameter  $D(\lambda)$  around the ZDWs of both conventional and highly nonlinear DSFs.

a careful spectral analysis of MI and DWs generated simply by use of a wavelength-tunable high-power fiber laser, this method is easy to implement and is able to retrieve dispersion parameters up to the fourth-order without extrapolation.

#### ACKNOWLEDGMENT

The authors thank T. Okuno from Sumitomo electric for helpful discussions and for providing the HNLF.

#### REFERENCES

- [1] S. E. Mechels, J. B. Schalger, and D. L. Franzen, "Accurate measurements of the zero-dispersion wavelength in optical fibers," *J. Res. Nat. Inst. Stand. Technol.*, vol. 102, pp. 333–347, 1997.
- [2] H. Chen, "Simultaneous measurements of non-linear coefficient, zero-dispersion wavelength and chromatic dispersion in dispersion-shifted fibers by four-wave mixing," *Opt. Commun.*, vol. 220, pp. 331–335, 2003.
- [3] C. Mazzali, D. F. Grosz, and H. L. Fragnito, "Simple method for measuring dispersion and nonlinear coefficient near the zero-dispersion wavelength of optical fibers," *IEEE Photon. Technol. Lett.*, vol. 11, no. 2, pp. 251–253, Feb. 1999.
- [4] G. Wong, A. Chen, S. Ha, R. Kruhlak, S. Murdoch, R. Leonhardt, J. Harvey, and N. Joly, "Characterization of chromatic dispersion in photonic crystal fibers using scalar modulation instability," *Opt. Express*, vol. 13, pp. 8662–8670, 2005.
- [5] J. Fatome, S. Pitois, and G. Millot, "Measurement of nonlinear and chromatic dispersion parameters of optical fibers using modulation instability," *Opt. Fiber. Technol.*, 2006, to be published.
- [6] A. Mussot, E. Lantz, H. Maillotte, C. Finot, S. Pitois, and T. Sylvestre, "Spectral broadening of a partially coherent CW optical beam in single-mode fibers," *Opt. Express*, vol. 12, pp. 2838–2843, 2004.
- [7] G. P. Agrawal, "Nonlinear fiber optics," in *Optics and Photonics*, 3rd ed. San Diego, CA: Academic, 2001.
- [8] S. Pitois and G. Millot, "Experimental observation of a new modulational instability spectral window induced by fourth-order dispersion in a normally dispersive single-mode optical fiber," *Opt. Commun.*, vol. 226, pp. 415–422, 2003.
- [9] M. E. Marhic, K. K.-Y. Wong, and L. G. Kazovsky, "Wide-band tuning of the gain spectra of one-pump fiber optical parametric amplifiers," *IEEE J. Sel. Topics Quantum Electron.*, vol. 10, no. 5, pp. 1133–1141, Sep./Oct. 2004.
- [10] J. Harvey, R. Leonhardt, S. Coen, G. Wong, J. Knight, W. Wadsworth, and P. St. J. Russell, "Scalar modulation instability in the normal dispersion regime by use of a photonic crystal fiber," *Opt. Lett.*, vol. 28, pp. 2225–2227, 2003.
- [11] P. K. A. Wai, C. R. Menyuk, H. H. Chen, and Y. C. Lee, "Soliton at the zero-dispersion wavelength of a single-mode fiber," *Opt. Lett.*, vol. 12, pp. 628–630, 1987.
- [12] N. Akhmediev and M. Karlsson, "Cherenkov radiation emitted by solitons in optical fibers," *Phys. Rev. A*, vol. 51, pp. 2602–2607, 1995.